Macromolecules **2000,** *33,* 3543−3549

Living Radical Polymerization of Styrene by Half-Metallocene Iron Carbonyl Complexes[1]

Yuzo Kotani, Masami Kamigaito, and Mitsuo Sawamoto*

Department of Polymer Chemistry, Graduate School of Engineering, Kyoto University, Kyoto 606-8501, Japan

Received November 29, 1999; Revised Manuscript Received March 21, 2000

ABSTRACT: A series of half-metallocene Fe(II) complexes [$FeLX(CO)_2$; X = I, Br; L = η^5-C_5H_5 (Cp), η^5-C_5Me_5 (Cp*)] were employed for living radical polymerization of styrene in conjunction with halide initiators [$(CH_3)_2C(CO_2Et)X$; X = I and Br] in the presence or absence of Ti(O*i*-Pr)$_4$. The iron-based systems induced living radical polymerization of styrene to give polymers of narrow molecular weight distributions (MWDs) in the presence of Ti(O*i*-Pr)$_4$. The Cp*−iodide complex [$FeCp^*I(CO)_2$] gave the narrowest MWDs ($\bar{M}_w/\bar{M}_n$ = 1.05−1.09) when coupled with the iodoester initiator. The polymerization with $FeCpI(CO)_2$ was examined in several ether solvents, where dioxane proved most effective. Dinuclear iron(I) complexes [$Fe_2Cp_2(CO)_4$] were also employed for living radical polymerization of styrene coupled with the iodoester initiator. Dinuclear half-metallocenes induced faster living polymerization even without Ti(O*i*-Pr)$_4$. Cyclic voltammetric analysis showed that the redox potential of the dinuclear complex is lower than that of the mononuclear one. Some interactions of Ti(O*i*-Pr)$_4$ with the iron complexes were observed by cyclic voltammetric and NMR analysis of the mixtures.

Introduction

Living radical polymerization is now one of the most rapidly developing areas in polymer chemistry in the past several years, still expanding the scope of initiating/catalyst systems, applicable monomers, and novel polymer structures to be obtained thereby.[2] Transition-metal catalysts have been effectively used for living radical polymerization (Scheme 1), where the dormant carbon−halogen bond at a polymer terminal is reversibly and homolytically cleaved by the transition metal complexes, such as $\sim\sim\sim C{-}X + M(n) \rightleftarrows \sim\sim\sim C^{\bullet}\ X{-}M(n{+}1)$. Along with the nitroxide-mediated[2a,c] and RAFT counterparts,[3] the metal-mediated living radical polymerization is one of the most efficient systems in terms of versatility and controllability. One of its distinguishable features is that metal catalysts can be designed according to monomers and other conditions, in contrast to the other systems where the dormant covalent bonds are cleaved not by catalysts but by heat or carbon radical species.

The effective transition metal catalysts thus far employed for the living radical polymerizations are mostly halides of metals such as Ru,[4−9] Cu,[10−15] Fe,[16,17] Ni,[18−21] Rh,[22−24] Pd,[25] Re,[26] and Mo[27,28] with phosphine- or nitrogen-based ligands. These metal complexes most probably undergo reversible one-electron redox reaction by interacting catalytically with organic halides to form radical growing species. Obviously, the design of catalysts by the central metals and the ligands is crucial for the activity and the controllability of the metal-catalyzed polymerization.

Among the metals, iron is especially attractive because of its low cost and harmlessness. Recently, we first developed an iron-mediated living radical polymerization of methyl methacrylate (MMA) with the use of Fe(II) phosphine halides, $FeX_2(PPh_3)_2$ (X = Cl, Br).[16] Similar living polymerizations of MMA and styrene were also achieved by a mixture of FeX_2 (X = Cl, Br) and phosphine- or nitrogen-based compounds.[17] These showed that, if properly designed, iron complexes can be suitable catalysts for transition metal catalyzed living radical polymerization.[29] Later on, however, studies on iron catalysts have not been extensively done in comparison to copper and ruthenium derivatives. Quite recently, we have found that a half-metallocene-type iron complex, $FeCpI(CO)_2$, led to living radical polymerization of styrene in the presence of an iodide initiator and Ti(O*i*-Pr)$_4$ as an additive to give polymers of precisely controlled molecular weights and narrow molecular weight distributions (MWDs) ($\bar{M}_w/\bar{M}_n \sim 1.1$).[30] Such a half-metallocene iron carbonyl complex can be directly modified by anionic Cp-based ligands, which coordinate to the iron center more tightly than neutral phosphines or amines, so as to be more active and more efficient in contrast to simple iron complexes such as $FeX_2(PPh_3)_2$. Cp-based ligands proved also effective in increasing the catalytic activity and the controllability of the polymerization in the Ru(II)-based living radical polymerizations.[7]

Scheme 1. Living Radical Polymerization of Styrene with Fe(II) Complexes

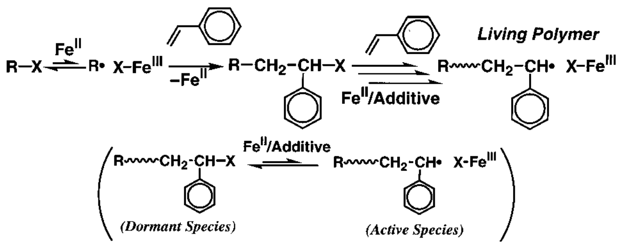

In this study, a series of half-metallocene iron(II) carbonyl complexes [$FeLX(CO)_2$; L = Cp, Cp* (Cp* = η^5-C_5Me_5); X = I, Br] were employed for polymerization of styrene coupled with a halide initiator [$(CH_3)_2C(CO_2Et)X$; X = I, Br] in the presence of Ti(O*i*-Pr)$_4$, where effects of Cp-based ligands and halogens were studied (Scheme 2). These iron carbonyl complexes are moisture- and oxygen-tolerant and thus can be prepared under air by halogenation of the corresponding dinuclear iron(I) carbonyl complexes [$Fe_2L_2(CO)_4$; L = Cp,

10.1021/ma991990f CCC: $19.00

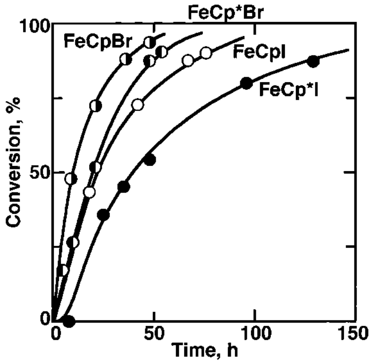

Figure 1. Living radical polymerization of styrene with $(CH_3)_2C(CO_2Et)X$/Fe(II) in the presence of Ti(O*i*-Pr)$_4$ in toluene at 80 °C: $[styrene]_0 = 6.0$ M; $[(CH_3)_2C(CO_2Et)X]_0 = 60$ mM; $[Fe(II)]_0 = 10$ mM; $[Ti(Oi\text{-}Pr)_4]_0 = 100$ mM. $(CH_3)_2C(CO_2Et)Br$/FeCpBr (◑), $(CH_3)_2C(CO_2Et)Br$/FeCp*Br (◐), $(CH_3)_2C(CO_2Et)I$/FeCpI (○), $(CH_3)_2C(CO_2Et)I$/FeCp*I (●).

Scheme 2. Various Half-Metallocene-Type Fe Complexes for Living Radical Polymerization of Styrene

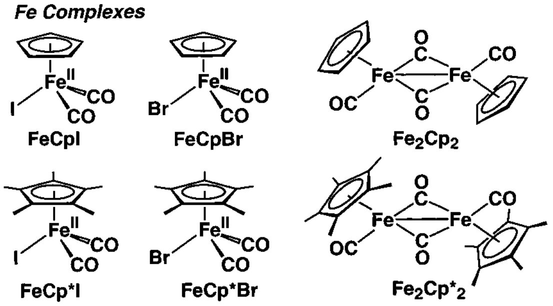

Cp*].[31,32] These dinuclear complexes were also examined herein as possible catalysts for living radical polymerization of styrene. Prior to our work on living radical polymerizations, halogen-free iron carbonyl complexes such as $Fe_2Cp_2(CO)_4$,[33,34] $Fe_2(CO)_9$,[35] and $Me_3NFe(CO)_4$[35] have proved effective in metal-mediated radical addition or Kharasch reactions between organic halides and olefins. This work revealed that $Fe_2L_2(CO)_4$ induced living radical polymerization of styrene without additives such as Ti(O*i*-Pr)$_4$. Effects of ligands and Ti(O*i*-Pr)$_4$ along with catalytic activity were investigated by cyclic voltammetry and NMR spectroscopy.

Results and Discussion

1. Half-Metallocene Fe(II) Complexes: FeLX(CO)$_2$ (X = I, Br; L = Cp, Cp*). As we reported previously, FeCpI(CO)$_2$ induced living radical polymerization of styrene, when coupled with $(CH_3)_2C(CO_2Et)I$ (initiator) and Ti(O*i*-Pr)$_4$ (additive) in toluene at 80 °C.[30] A series of half-metallocene complexes [FeLX(CO)$_2$: FeCpBr (L = Cp, X = Br); FeCp*Br (L = Cp*, X = Br); FeCpI (L = Cp, X = I); FeCp*I (L = Cp*, X = I)] were synthesized[31,32] and employed for the polymerization of styrene (Figure 1). For the iodide complexes, an iodoester initiator [$(CH_3)_2C(CO_2Et)I$] was used, and a bromoester [$(CH_3)_2C(CO_2Et)Br$] was used for the bromide complexes to avoid the formation of mixed-halogen terminals and complexes.[6] The polymerization rate depended on the halogens and the ligands of catalysts and increased in the following order: FeCp*I < FeCpI < FeCp*Br < FeCpBr. Thus, a more electron-donating ligand, Cp*, led to a slower polymerization for both bromide and iodide complexes. The polymerizations with two bromide complexes were faster than those with the iodides.

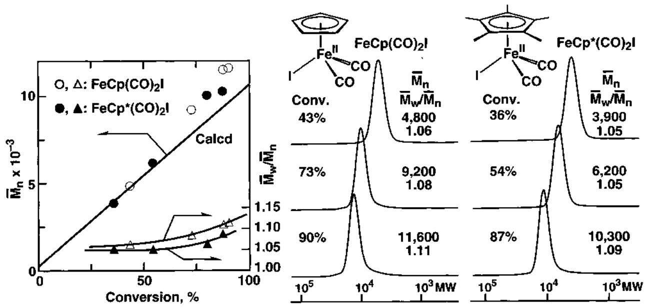

Figure 2. $\bar{M}_n$, $\bar{M}_w/\bar{M}_n$, and MWD curves of polystyrene obtained with $(CH_3)_2C(CO_2Et)I$/Fe(II) in the presence of Ti(O*i*-Pr)$_4$ in toluene at 80 °C: $[styrene]_0 = 6.0$ M; $[(CH_3)_2C(CO_2Et)I]_0 = 60$ mM; $[Fe(II)]_0 = 10$ mM; $[Ti(Oi\text{-}Pr)_4]_0 = 100$ mM. FeCpI (○, △), FeCp*I (●, ▲).

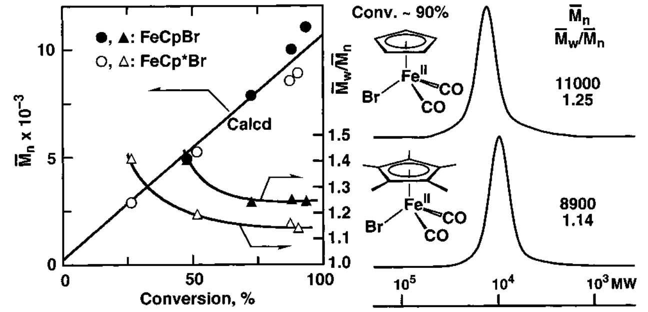

Figure 3. $\bar{M}_n$, $\bar{M}_w/\bar{M}_n$, and MWD curves of polystyrene obtained with $(CH_3)_2C(CO_2Et)Br$/Fe(II) in the presence of Ti(O*i*-Pr)$_4$ in toluene at 80 °C: $[styrene]_0 = 6.0$ M; $[(CH_3)_2C(CO_2Et)Br]_0 = 60$ mM; $[Fe(II)]_0 = 10$ mM; $[Ti(Oi\text{-}Pr)_4]_0 = 100$ mM. FeCpBr (●, ▲), FeCp*Br (○, △).

Figure 2 shows the $\bar{M}_n$, $\bar{M}_w/\bar{M}_n$, and size-exclusion chromatography (SEC) traces of the polystyrene obtained with FeCpI and FeCp*I. With both complexes, the $\bar{M}_n$ increased in direct proportion to monomer conversion and agreed well with the calculated values based on the assumption that one molecule of iodide initiator generated one living chain. The MWDs stayed very narrow with the iodide-based systems, especially with FeCp*I ($\bar{M}_w/\bar{M}_n = 1.05-1.09$).

A similar trend was observed in the polymerization with the bromide complexes (Figure 3). The $\bar{M}_n$ were precisely controlled and agreed well with calculated values with both FeCpBr and FeCp*Br, where the MWDs narrowed as the polymerization proceeded. In theses bromine-based initiating systems, the MWDs with the Cp* complex were also narrower than those with the Cp complex.

These results show that the MWDs became narrower in the following order of $\bar{M}_w/\bar{M}_n$ ratio: FeCpBr (≥ 1.25); FeCp*Br (≥ 1.14); FeCpI (1.06−1.11); FeCp*I (1.05−1.09). In a polymerization involving the equilibrium between dormant and active species, in general, the MWD of polymers is determined by the rates of propagation and dormant-active species interconversion: a faster interconversion and/or a slower polymerization results in a narrower MWD. As denoted in Scheme 1, a single electron must be transferred from Fe(II) to the dormant polymer terminal. Among our four iron complexes, the electron density of the Fe(II) center is considered the highest for FeCp*I due to the more electron-donating Cp* ligand and the less electron-withdrawing iodo group. Such an electron-rich complex

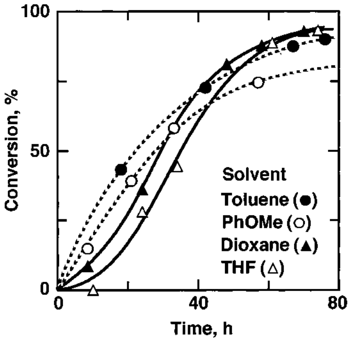

Figure 4. Living radical polymerization of styrene with $(CH_3)_2C(CO_2Et)I/FeCpI/Ti(Oi\text{-}Pr)_4$ in toluene (●), PhOMe (○), dioxane (▲), and THF (△) at 80 °C: $[styrene]_0 = 6.0$ M; $[(CH_3)_2C(CO_2Et)I]_0 = 60$ mM; $[FeCpI]_0 = 10$ mM; $[Ti(Oi\text{-}Pr)_4]_0 = 100$ mM.

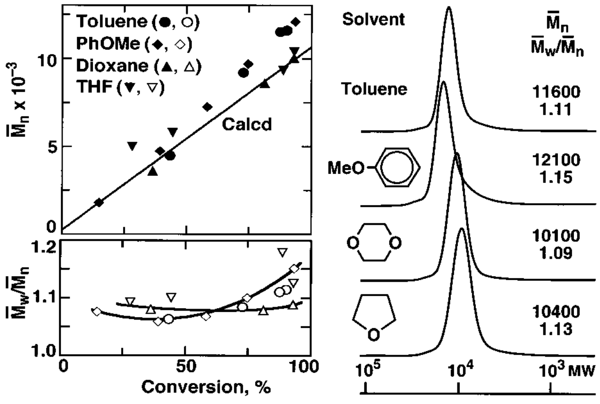

Figure 5. $\bar{M}_n$, $\bar{M}_w/\bar{M}_n$, and MWD curves of polystyrene obtained with $(CH_3)_2C(CO_2Et)I/FeCpI/Ti(Oi\text{-}Pr)_4$ in toluene (●, ○), PhOMe (◆, ◇), dioxane (▲, △), and THF (▼, ▽) at 80 °C: $[styrene]_0 = 6.0$ M; $[(CH_3)_2C(CO_2Et)I]_0 = 60$ mM; $[FeCpI]_0 = 10$ mM; $[Ti(Oi\text{-}Pr)_4]_0 = 100$ mM.

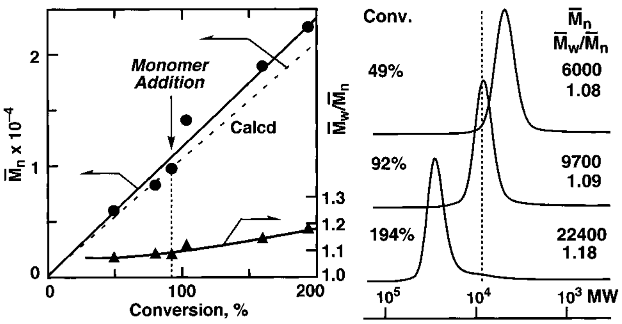

Figure 6. $\bar{M}_n$ (●), $\bar{M}_w/\bar{M}_n$ (▲), and MWD curves of polystyrene obtained in a monomer-addition experiment with $(CH_3)_2C(CO_2Et)I/FeCpI/Ti(Oi\text{-}Pr)_4$ in dioxane at 80 °C: $[styrene]_0 = 6.0$ M; $[(CH_3)_2C(CO_2Et)I]_0 = 60$ mM; $[FeCpI]_0 = 10$ mM; $[Ti(Oi\text{-}Pr)_4]_0 = 100$ mM. The diagonal dashed line indicates the calculated $\bar{M}_n$ assuming the formation of one living polymer per $(CH_3)_2C(CO_2Et)I$ molecule.

Scheme 3. Kharasch Addition Reaction with $Fe_2Cp_2(CO)_4$

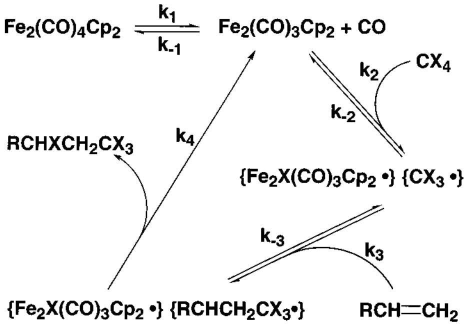

facilitates electron release to induce faster interconversion. The lower bond energy of the C−I terminal is also effective in narrowing MWD.[36] The polymerization with FeCp*I was slowest among them, which also produces the narrowest MWDs. The slower the polymerization, the narrower the MWD. Thus, a series of half-metallocene Fe(II) complexes induced living radical polymerization of styrene, and an electron-donating Cp* ligand provided more precise polymerization control.

2. Solvent Effects on Living Radical Polymerization of Styrene with FeCpI. Apart from toluene, various ethers [anisole (PhOMe), dioxane, and tetrahydrofuran (THF)] were examined as a solvent for living radical polymerizations of styrene with $(CH_3)_2C(CO_2Et)I$ and FeCpI in the presence of $Ti(Oi\text{-}Pr)_4$ at 80 °C (Figure 4). In all solvents, polymerizations proceeded, although slight induction periods were observed in dioxane and THF. The polymerizations in dioxane and THF reached high conversion (~90%) faster than in toluene and PhOMe: dioxane (93% in 70 h); THF (93% in 74 h), toluene (90% in 76 h); PhOMe (93% in 124 h).

Figure 5 shows $\bar{M}_n$, $\bar{M}_w/\bar{M}_n$, and SEC curves of the obtained polystyrenes in the ether solvents. In dioxane, the $\bar{M}_n$ agreed well with the calculated values, and the MWDs were narrower than those obtained in the other solvents. In THF the $\bar{M}_n$ were controlled, although the MWDs were slightly broader. The polymerization in PhOMe was similar to that in toluene where the $\bar{M}_n$ were slightly higher than the calculated values. These results suggest that less bulkier ether solvents such as dioxane and THF interact or coordinate to the iron complex, which affects the activity or the stability of the complex.

Monomer-addition experiments were carried out in dioxane with $(CH_3)_2C(CO_2Et)I/FeCpI(CO)_2/Ti(Oi\text{-}Pr)_4$ at 80 °C (Figure 6). A fresh feed of styrene was added to the reaction mixture after the polymerization was virtually completed. The second-phase polymerization further proceeded to reach 194% monomer conversion in an additional 144 h. The $\bar{M}_n$ increased in direct proportion to monomer conversion and agreed well with the calculated values, where the MWDs remained still narrow ($\bar{M}_w/\bar{M}_n = 1.18$). In similar monomer-addition experiments in toluene, however, a little shoulder was observed in SEC curve of the polystyrene obtained after monomer addition, along with slightly broader main MWDs (174% in additional 116 h; $\bar{M}_n = 25\,300$; $\bar{M}_w/\bar{M}_n = 1.38$). These results confirm the living nature of the $FeCpI(CO)_2$-based system in dioxane solvent.

3. Dinuclear Half-Metallocene Iron Complexes: $Fe_2Cp_2(CO)_4$ and $Fe_2Cp^*{}_2(CO)_4$. As mentioned in the Introduction, the dinuclear iron half-metallocene complex $Fe_2Cp_2(CO)_4$ (Fe_2Cp_2) is an effective catalyst for homogeneous Kharasch addition reaction (Scheme 3). An active catalyst is supposed to be an Fe(I) dinuclear complex, $Fe_2Cp_2(CO)_3$, which is formed via elimination of one of the carbonyl ligands from the tetrakis precursor.

We have thus employed $Fe_2Cp_2(CO)_4$ for living radical polymerization of styrene under the same condition performed with FeCpI: styrene was polymerized with Fe_2Cp_2 and $(CH_3)_2C(CO_2Et)I$ in the presence of $Ti(Oi\text{-}Pr)_4$ in dioxane at 80 or 60 °C (Figure 7). At both temperatures, polymerizations occurred smoothly to near

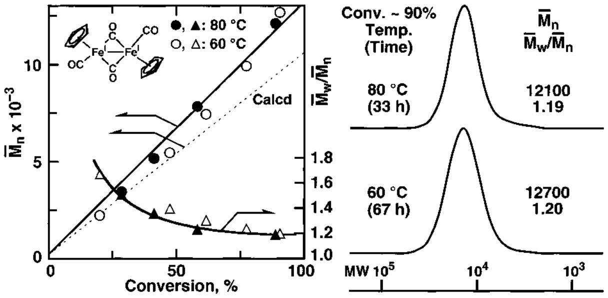

Figure 7. $\bar{M}_n$, $\bar{M}_w/\bar{M}_n$, and MWD curves of polystyrene obtained with $(CH_3)_2C(CO_2Et)I/Fe_2Cp_2$ in the presence of $Ti(Oi\text{-}Pr)_4$ in toluene at 80 °C (●, ▲) and 60 °C (○, △): $[styrene]_0 = 6.0$ M; $[(CH_3)_2C(CO_2Et)Br]_0 = 60$ mM; $[Fe_2Cp_2]_0 = 10$ mM; $[Ti(Oi\text{-}Pr)_4]_0 = 100$ mM. The diagonal dashed line indicates the calculated $\bar{M}_n$ assuming the formation of one living polymer per $(CH_3)_2C(CO_2Et)I$ molecule.

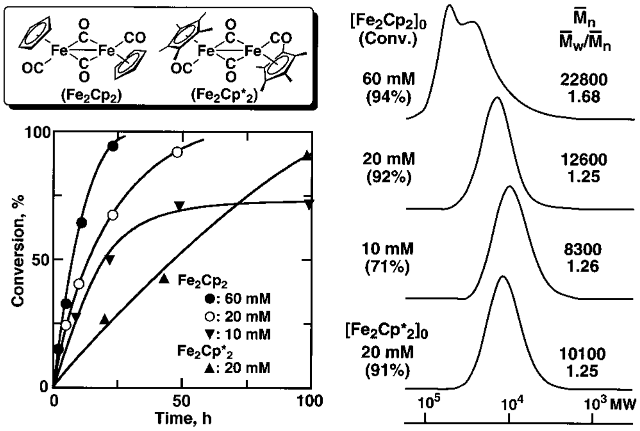

Figure 8. Living radical polymerization of styrene with $(CH_3)_2C(CO_2Et)I$/Fe complexes in dioxane at 60 °C: $[styrene]_0 = 6.0$ M; $[(CH_3)_2C(CO_2Et)I]_0 = 60$ mM; $[Fe_2Cp_2]_0 = 60$ mM (●), 20 mM (○), and 10 mM (▼); $[Fe_2Cp^*_2]_0 = 10$ mM (▲).

completion in 33 h (80 °C) or 67 h (60 °C), which were much faster than the polymerizations with FeCpI otherwise under the same conditions (cf. Figure 4). The $\bar{M}_n$ of the obtained polystyrene increased in direct proportion to monomer conversion and almost agreed with the calculated values, where the MWDs were fairly narrow ($\bar{M}_w/\bar{M}_n \sim 1.2$). Thus, living polymerization can also be achieved with the dinuclear iron complex in the presence of $Ti(Oi\text{-}Pr)_4$.

We have also employed Fe_2Cp_2 in the absence of $Ti(Oi\text{-}Pr)_4$: styrene was polymerized with Fe_2Cp_2 and $(CH_3)_2C(CO_2Et)I$ in dioxane at 60 °C (Figure 8). A smooth polymerization proceeded to reach 94% conversion in 23 h at a high initial concentration of the iron complex, $[Fe_2Cp_2]_0 = 60$ mM. The lower the $[Fe_2Cp_2]_0$ concentration, the slower the polymerization; e.g., at $[Fe_2Cp_2]_0 = 10$ mM, monomer conversion leveled off around 75%. The SEC curves obtained at $[Fe_2Cp_2]_0 = 60$ mM showed bimodal distributions, where the $\bar{M}_n$ were much higher than the calculated values, although they were narrow and unimodal at lower conversions (≤60%). The SEC peak molecular weight for the higher molecular weight fraction was 55 000, almost twice the lower (28 800) which was most likely due to the coupling reaction of polystyryl radicals at such high conversions of styrene. At $[Fe_2Cp_2]_0 = 20$ mM, on the other hand, the MWDs were unimodal and relatively narrow ($\bar{M}_w/\bar{M}_n \sim 1.2$), and the $\bar{M}_n$ increased in direct proportion to monomer conversion and almost agreed with the calculated values. Another dinuclear iron(I) complex, $Fe_2Cp^*_2(CO)_4$ ($Fe_2Cp^*_2$), also gave relatively narrow MWDs ($\bar{M}_w/\bar{M}_n = 1.25$). Thus, half-metallocene-type dinuclear complexes induced living polymerization of styrene without any additives, although the polymerization conditions were carefully selected.

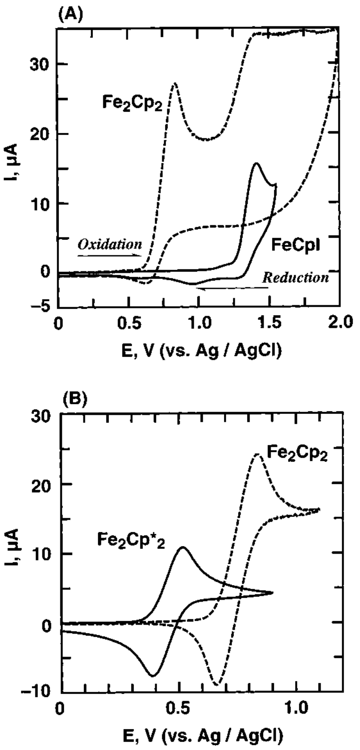

Figure 9. Cyclic voltammograms (0.1 V s^{-1}) of Fe complexes (5 mM) in CH_2ClCH_2Cl at 30 °C: $[n\text{-}Bu_4NPF_6] = 100$ mM (supporting electrolyte). (A) FeCpI (solid line) and Fe_2Cp_2 (dashed line). (B) Fe_2Cp_2 (dashed line) and $Fe_2Cp^*_2$ (<5 mM, because of solubility) (solid line).

4. Cyclic Voltammetry of Fe Complexes. The electrochemical behavior of the Fe complexes was then examined by cyclic voltammetry, which should give information about the redox processes of the complexes. All the measurements were conducted in CH_2ClCH_2Cl containing $n\text{-}Bu_4NPF_6$ (0.1 M) at a platinum working electrode with a scan rate of 0.1 V s^{-1}. Cyclic voltammograms of FeCpI and Fe_2Cp_2 are shown in Figure 9A.

FeCpI showed an oxidation wave around 1.4 V but almost no reduction wave (solid line in Figure 9A). Such a high oxidation potential (~1.4 V) of FeCpI suggests that FeCpI alone is not a good catalyst for the living polymerization as reported.[30]

Fe_2Cp_2 showed two oxidation waves when the potential was raised to 2.0 V (dashed line in Figure 9A). The lower potential peak is assigned to one-electron oxidation of one of the two Fe(I) centers in the dinuclear complex [Fe(I, I) → Fe(I, II)], and the second peak is due to the oxidation of the other nucleus [Fe(I, II) → Fe(II, II)]. The cyclic voltammogram for the first scan showed small reduction wave around 0.7 V, which corresponds to the reduction of Fe(I, II) to Fe(I, I), although the second scan gave no waves. These show that the oxidation of Fe(I, II) to Fe(II, II) is chemically irreversible, probably due to decomposition of the compound after the second electrochemical oxidation. However, a quasi-reversible wave for Fe(I/II) couple ($\Delta E = E_{p,a} - E_{p,c} = 176$ mV; $E_{p,a}$ and $E_{p,c}$ are peak potential of the oxidation and reduction waves, respectively) was observed at $E_{1/2} = (E_{p,a} + E_{p,c})/2 = 749$ mV when the

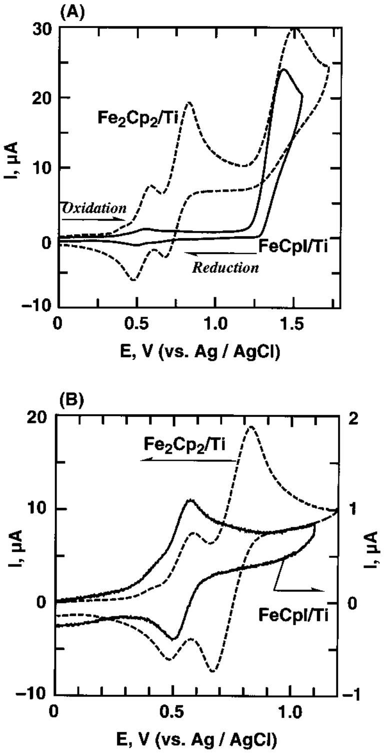

Figure 10. Cyclic voltammograms (0.1 V s^{-1}) of Fe complex/Ti(O*i*-Pr)$_4$ (5/15 mM; aged at 80 °C for 24 h just before measurement) in CH_2ClCH_2Cl at 30 °C: [*n*-Bu_4NPF_6] = 100 mM (supporting electrolyte). (A) FeCpI/Ti(O*i*-Pr)$_4$ (solid line) and Fe_2Cp_2/Ti(O*i*-Pr)$_4$ (dashed line). (B) FeCpI/Ti(O*i*-Pr)$_4$ (solid line) and Fe_2Cp_2/Ti(O*i*-Pr)$_4$ (dashed line) (sweep range: 0−1.1 or 1.2 V).

scanning was turned to reduction direction at 1.1 V, where the first oxidation [Fe(I, I) → Fe(I, II)] was observed (dashed line in Figure 9B). This redox cycle was highly reproducible in several scans in the range 0−1.1 V vs Ag/AgCl. This shows that Fe_2Cp_2 undergoes a chemically reversible redox reaction between Fe(I, I) and Fe(I, II). It follows that the dinuclear complex induces living radical polymerization via such a redox cycle even in the absence of Ti(O*i*-Pr)$_4$. $Fe_2Cp^*_2$ was also analyzed to give similar quasi-reversible cycle at $E_{1/2}$ = 451 mV (ΔE = 130 mV), lower than that of Fe_2Cp_2 (solid line in Figure 9B). This indicates that a more electron-donating ligand, Cp*, lowers the oxidation potential of the Fe complex.

Cyclic voltammograms of FeCpI and Fe_2Cp_2 in conjunction with Ti(O*i*-Pr)$_4$ were then measured. In these experiments the Fe complex was mixed with Ti(O*i*-Pr)$_4$ in CH_2ClCH_2Cl. The solution was heated to 80 °C, kept at the temperature for 24 h, and cooled to 30 °C. Finally, an *n*-Bu_4NPF_6 solution of CH_2ClCH_2Cl was added to the mixture. The solid line in Figure 10A shows the voltammogram of an FeCpI/Ti(O*i*-Pr)$_4$ (5/15 mM) mixture, while the dashed one for Fe_2Cp_2/Ti(O*i*-Pr)$_4$ (5/15 mM). FeCpI/Ti(O*i*-Pr)$_4$ showed small oxidation and reduction waves at 0.56 and 0.50 V ($E_{1/2}$ = 530 mV), respectively, in addition to the oxidation wave at 1.35 V which was also observed for FeCpI alone (cf. Figure 9). The peaks are probably due to the new redox potential of FeCpI modified with Ti(O*i*-Pr)$_4$. Fe_2Cp_2/Ti(O*i*-Pr)$_4$ also exhibited a new redox wave at nearly the same potential ($E_{1/2}$ = 534 mV), in addition to the peaks observed for the complex alone (Figure 9A). It is also noteworthy that the redox cycle for Fe_2Cp_2 was reproducible after several scans even in such a wide voltage range (0 to ~1.7 V), in contrast to the results for in the absence of Ti(O*i*-Pr)$_4$ (cf. Figure 9A). This may indicate that the Fe center can undergo chemically reversible redox reactions due to the stabilization of higher oxidation states by Ti(O*i*-Pr)$_4$. Similar stabilizing effects of alkoxide additives were observed with $RuCl_2(PPh_3)_3$ in the presence of Al(O*i*-Pr)$_3$.[37] This is consistent with the polymerization results where Fe_2Cp_2 led to a fast living polymerization at its lower concentration in the presence of Ti(O*i*-Pr)$_4$ (Figure 7). Thus, added Ti(O*i*-Pr)$_4$ probably forms a new complex with FeCpI and Fe_2Cp_2 and/or stabilizes iron species at higher oxidation states.

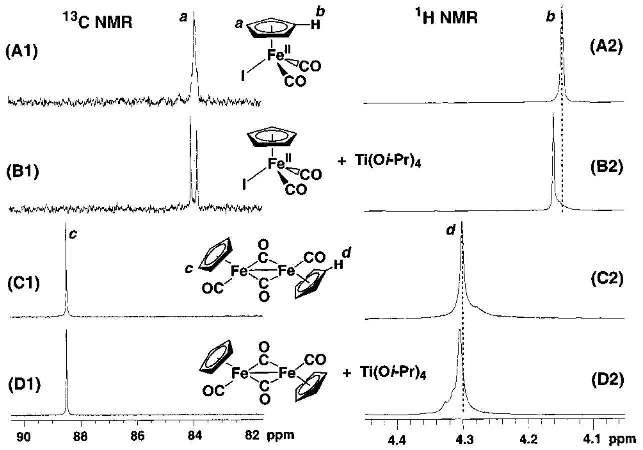

Figure 11. ^{13}C and ^{1}H NMR spectra of the mixtures of Fe complex and Fe complex/Ti(O*i*-Pr)$_4$ in toluene-d_8 at 80 °C: [Fe complex]$_0$/[Ti(O*i*-Pr)$_4$]$_0$ = 80/80 mM. FeCpI (A1, A2), FeCpI/Ti(O*i*-Pr)$_4$ (B1, B2), Fe_2Cp_2 (C1, C2), Fe_2Cp_2/Ti(O*i*-Pr)$_4$ (D1, D2).

Figure 10B shows the voltammograms of the mixtures in a narrower scan range (0 to 1.1 or 1.2 V). Fe_2Cp_2/Ti(O*i*-Pr)$_4$ gave the redox cycles at $E_{1/2}$ = 537 and 750 mV(ΔE = 97 and 157 mV, respectively), one of which was very similar to that of FeCpI/Ti(O*i*-Pr)$_4$ ($E_{1/2}$ = 534 mV, ΔE = 75 mV). Both redox cycles were reproducible. In the presence of Ti(O*i*-Pr)$_4$, FeCpI is most probably transformed into an effective catalyst that involves a new redox cycle with a low oxidation/reduction potential. However, the peak intensity was very small, which resulted in a slower polymerization with FeCpI/Ti(O*i*-Pr)$_4$. Thus, cyclic voltammetric analysis gave us valuable information on the complexes, although the interaction between the Fe complexes and Ti(O*i*-Pr)$_4$ was not fully clarified yet.

5. NMR Analysis. Possible interaction between the Fe complexes and Ti(O*i*-Pr)$_4$ was analyzed by ^{13}C and ^{1}H NMR spectroscopy. The analyses were carried out in toluene-d_8 at 80 °C, where mixtures of the complex and Ti(O*i*-Pr)$_4$ were preheated at 80 °C for 24 h. Figure 11 shows ^{13}C and ^{1}H NMR spectra of FeCpI (A1, A2), FeCpI/Ti(O*i*-Pr)$_4$ (B1, B2), Fe_2Cp_2 (C1, C2), and Fe_2Cp_2/Ti(O*i*-Pr)$_4$ (D1, D2). The ^{13}C signal *a* at 83.89 ppm in Figure 9-A1 is attributed to the aromatic carbon of the Cp ring in FeCpI, and its proton *b* was observed at 4.14 ppm (A2). On addition of Ti(O*i*-Pr)$_4$, peak *a* split into two sharp signals (B1) and peak *b* shifted downfield (4.16 ppm in B2). Apparently, Ti(O*i*-Pr)$_4$ interacted with FeCpI, though the ^{13}C chemical shift of the carbonyl group did not change (213.8 ppm). On the other hand, almost no change was observed for Fe_2Cp_2 on addition of Ti(O*i*-Pr)$_4$. The Cp carbon was observed at 88.49 ppm as a sharp singlet both in the absence and in the presence of Ti(O*i*-Pr)$_4$ (Figure 9-C1 and D1). A very slight downfield shift was observed on ^{1}H NMR spectra (C2 and D2).

These results are consistent with the polymerization behavior. The FeCpI-based system induced a slow living polymerization in the presence of Ti(O*i*-Pr)$_4$, but fast and uncontrolled oligomerization occurred without Ti(O*i*-Pr)$_4$. The NMR analysis indicate that Ti(O*i*-Pr)$_4$ changes FeCpI into another iron species that is active for living polymerization. On the other hand, the Fe$_2$Cp$_2$-based system induced living polymerization with and without Ti(O*i*-Pr)$_4$. Significant changes in NMR spectra by addition of Ti(O*i*-Pr)$_4$ were not observed for Fe$_2$Cp$_2$. This probably suggests that the dinuclear complex seems as an active catalyst without significant changes in its structure via interaction with Ti(O*i*-Pr)$_4$. However, Ti(O*i*-Pr)$_4$ may prevent the decomposition of Fe$_2$Cp$_2$, because the polymerization at low concentration of Fe$_2$Cp$_2$ became slower without Ti(O*i*-Pr)$_4$ as the polymerization proceeded.

In conclusion, living radical polymerization of styrene was achieved with a series of half-metallocene iron complexes, FeCpBr, FeCp*Br, FeCpI, and FeCp*I in the presence of Ti(O*i*-Pr)$_4$; the FeCp*I seems the best among the four. Polymerization rate and MWDs depend on the structure of the iron complexes, where an electron-donating ligand such as Cp* slows the polymerization and narrows the MWDs. FeCp*I gave the narrowest MWDs ($\bar{M}_w/\bar{M}_n = 1.05-1.09$) coupled with iodo initiator. As solvent, dioxane proved better than toluene in controlling the polymerization. Dinuclear iron complexes, Fe$_2$Cp$_2$ and Fe$_2$Cp*$_2$, induced faster living radical polymerization even in the absence of Ti(O*i*-Pr)$_4$. Cyclic voltammetric studies revealed that the dinuclear complex has a lower redox potential than the mononuclear halide complex and that Ti(O*i*-Pr)$_4$ probably stabilizes iron species at higher oxidation states. These iron-based initiating systems recently proved equally active for acrylates, and block and random copolymerizations of styrene and acrylates were successful.[38]

Experimental Section

Materials. Styrene (Wako Chemicals; purity > 99%) was dried overnight over anhydrous sodium sulfate and distilled twice over calcium hydride under reduced pressure before use. All transition metal complexes were handled in a glovebox (M. Braun) under dry (<1.0 ppm) and oxygen-free (<1.0 ppm) argon. Ti(O*i*-Pr)$_4$ (Kanto Chemicals, >97%) was used as received. Toluene, dioxane (solvent), and tetralin (internal standard for gas chromatographic analysis of styrene) were dried overnight over calcium chloride, distilled twice over sodium benzophenone ketyl (toluene and dioxane) or calcium hydride (tetralin), and bubbled with dry nitrogen for more than 15 min immediately before use. Tetrahydrofuran (Wako Chemicals, infinity pure; purity > 99.8%) was dried for a few days over activated molecular sieves (4A) and bubbled with dry nitrogen for more than 15 min immediately before use. Anisole (Aldrich, anhydrous; purity = 99.7%) and toluene-d_8 (Aldrich; purity = 99.5%) were used as received.

Initiators. Ethyl 2-bromoisobutyrate [(CH$_3$)$_2$C(CO$_2$C$_2$H$_5$)Br] (Tokyo Kasei, purity > 98%) was distilled twice over calcium hydride under reduced pressure before use. Ethyl 2-iodoisobutyrate [(CH$_3$)$_2$C(CO$_2$C$_2$H$_5$)I] was prepared by the method of Curran et al.;[39] bp 50 °C/9 Torr; identified by 500 MHz ^{1}H NMR. Anal. Calcd for C$_6$H$_{11}$O$_2$I: C, 29.8; H, 4.58; I, 52.4. Found: C, 29.7; H, 4.59; I, 52.3.

Fe Complexes. FeCpI(CO)$_2$ (Aldrich; purity > 97%), Fe$_2$Cp$_2$(CO)$_4$ (Aldrich; purity > 99%), and Fe$_2$Cp*$_2$(CO)$_4$ (Azmax; purity > 95%) were used as received. FeCp*I(CO)$_2$ was synthesized by the method of King et al.[31] Anal. Calcd for C$_{12}$H$_{15}$O$_2$IFe: C, 38.54; H, 4.05; I, 33.93. Found: C, 38.32; H, 3.95; I, 33.92. FeCp*Br(CO)$_2$ and FeCpBr(CO)$_2$ were synthesized by the method of Fisher et al.[32] Anal. Calcd for C$_{12}$H$_{15}$O$_2$BrFe: C, 44.08; H, 4.62; Br, 24.44. Found: C, 43.98; H, 4.57; Br, 24.57. Calcd for C$_5$H$_5$O$_2$BrFe: C, 32.73; H, 1.96; Br, 31.11. Found: C, 32.66; H, 1.86; Br, 31.05.

Polymerization Procedures. Polymerization was carried out by the syringe technique under dry nitrogen in sealed glass tubes. A typical example for the polymerization of styrene with (CH$_3$)$_2$C(CO$_2$Et)I/FeCpI(CO)$_2$/Ti(O*i*-Pr)$_4$ is given below: FeCpI(CO)$_2$ (0.0122 g) was mixed with styrene (2.75 mL), dioxane (0.831 mL), and Ti(O*i*-Pr)$_4$ (0.118 mL), sequentially in this order. Immediately after adding toluene solution of (CH$_3$)$_2$C(CO$_2$Et)I (0.289 mL) into the reaction mixture, the solution was placed in an oil bath at 80 °C. The polymerization was terminated by cooling the reaction mixtures to −78 °C. Monomer conversion was determined from the concentration of residual monomer measured by gas chromatography with tetralin as the internal standard. The quenched reaction solutions were diluted with toluene (~20 mL) and rigorously shaken with an absorbent [Kyowaad-2000G-7 (Mg$_{0.7}$Al$_{0.3}$O$_{1.15}$); Kyowa Chemical] (~5 g) to remove the metal-containing residues. After the absorbent was separated by filtration (Whatman 113V), the filtrate was washed with water and evaporated to dryness to give the products, which were subsequently dried overnight.

Measurements. The MWD, $\bar{M}_n$, and $\bar{M}_w/\bar{M}_n$ ratios of the polymers were measured by size-exclusion chromatography (SEC) in chloroform at room temperature on three polystyrene gel columns (Shodex K-805L × 3) that were connected to a Jasco PU-980 precision pump and a Jasco 930-RI refractive index and 970-UV ultraviolet detectors. The columns were calibrated against 11 standard polystyrene samples (Pressure Chemical; $\bar{M}_n = 580-1\,547\,000$; $\bar{M}_w/\bar{M}_n \leq 1.1$) as well as the monomer. Cyclic voltammograms were recorded by using a Hokuto Denko HZ-3000 apparatus. Measurements were carried out at 0.10 V s^{-1} in a CH$_2$ClCH$_2$Cl solution (5.0 mM) containing *n*-Bu$_4$NPF$_6$ (100 mM) as the supporting electrolyte under argon. A three-electrode cell was used which was equipped with a platinum disk as a working electrode, a platinum wire as a counter electrode, and an Ag/AgCl electrode as a reference. ^{1}H NMR spectra were recorded in CDCl$_3$ at 25 °C on a JEOL JNM-LA500 spectrometer, operating at 500.16 MHz. Polymers for ^{1}H NMR analysis were fractionated by preparative SEC (column: Shodex K-2002).

Acknowledgment. With appreciation M.S. and M.K. acknowledge the support from the New Energy and Industrial Technology Development Organization (NEDO) under the Ministry of International Trade and Industry (MITI), Japan, through the grant for “Precision Catalytic Polymerization” in the Project “Technology for Novel High-Functional Material” (fiscal 1996-2000). Y.K. is grateful to the Japan Society for the Promotion of Sciences (JSPS) for JSPS Research Fellowships for Young Scientists and also to the Ministry of Education, Science, Culture, and Sports, Japan, for the partial support of this work by the Grant-in-Aid for Scientific Research (No. 3370). The authors also thank T. Ando of our group for his assistance in the cyclic voltammetric analysis.

References and Notes

(1) This work was presented in part at the 218th ACS National Meeting, New Orleans, LA, Aug 1999: Kotani, Y.; Kamigaito, M.; Sawamoto, M. *Polym. Prepr. (Am. Chem. Soc., Div. Polym. Chem.)* **1999**, *40* (2), 468.

(2) For recent reviews on living radical polymerizations, see: (a) Georges, M. K.; Veregin, R. P. N.; Kazmaier, P. M.; Hamer, G. K. *Trends Polym. Sci.* **1994**, *2*, 66. (b) Davis, T. P.; Kukulj, D.; Haddleton, D. M.; Maloney, D. R. *Trends Polym. Sci.* **1995**, *3*, 365. (c) Malmström, E. E.; Hawker, C. J. *Macromol.*

Chem. Phys. **1998**, *199*, 823. (d) Sawamoto, M.; Kamigaito, M. *Trends Polym. Sci.* **1996**, *4*, 371. (e) Colombani, D. *Prog. Polym. Sci.* **1997**, *22*, 1649. (f) *Controlled Radical Polymerization;* Matyjaszewski, K., Ed.; ACS Symposium Series 685; American Chemical Society: Washington, DC, 1998. (g) Sawamoto, M.; Kamigaito, M. In *Synthesis of Polymers (Materials Science and Technology Series)*; Schlüter, A.-D., Ed.; Wiley-VCH: Weinheim, Germany, 1999; Chapter 6. (h) Sawamoto, M.; Kamigaito, M. *CHEMTECH* **1999**, *39* (6), 30.

(3) Chiefari, J.; Chong, Y. K.; Ercole, F.; Krstina, J.; Jeffery, J.; Le, T. P. T.; Mayadunne, R. T. A.; Meijs, G. F.; Moad, C. L.; Moad, G.; Rizzardo, E.; Thang, S. H. *Macromolecules* **1998**, *31*, 5559.

(4) Kato, M.; Kamigaito, M.; Sawamoto, M. *Macromolecules* **1995**, *28*, 1721.

(5) Ando, T.; Kato, M.; Kamigaito, M.; Sawamoto, M. *Macromolecules* **1996**, *29*, 1070.

(6) Ando, T.; Kamigaito, M.; Sawamoto, M. *Tetrahedron* **1997**, *53*, 15445.

(7) Takahashi, H.; Ando, T.; Kamigaito, M.; Sawamoto, M. *Macromolecules* **1999**, *32*, 3820.

(8) Takahashi, H.; Ando, T.; Kamigaito, M.; Sawamoto, M. *Macromolecules* **1999**, *32*, 6461.

(9) Simal, F.; Demonceau, A.; Noels, A. F. *Angew. Chem., Int. Ed. Engl.* **1999**, *38*, 538.

(10) Wang, J.-S.; Matyjaszewski, K. *J. Am. Chem. Soc.* **1995**, *117*, 5614.

(11) Wang, J.-S.; Matyjaszewski, K. *Macromolecules* **1995**, *28*, 7901.

(12) Patten, T. E.; Xia, J.; Abernathy, T.; Matyjaszewski, K. *Science* **1996**, *272*, 866.

(13) Percec, V.; Barboiu, B. *Macromolecules* **1995**, *28*, 7970.

(14) Percec, V.; Barboiu, B.; Kim, H.-J. *J. Am. Chem. Soc.* **1998**, *120*, 305.

(15) Haddleton, D. M.; Jasieczek, C. B.; Hannon, M. J.; Shooter, A. J. *Macromolecules* **1997**, *30*, 2190.

(16) Ando, T.; Kamigaito, M.; Sawamoto, M. *Macromolecules* **1997**, *30*, 4507.

(17) Matyjaszewski, K.; Wei, M.; Xia, J.; McDermott, N. E. *Macromolecules* **1997**, *30*, 8161.

(18) Granel, C.; Dubois, Ph.; Jérôme, R.; Teyssié, Ph. *Macromolecules* **1996**, *29*, 8576.

(19) Uegaki, H.; Kotani, Y.; Kamigaito, M.; Sawamoto, M. *Macromolecules* **1997**, *30*, 2249.

(20) Uegaki, H.; Kotani, Y.; Kamigaito, M.; Sawamoto, M. *Macromolecules* **1998**, *31*, 6756.

(21) Uegaki, H.; Kamigaito, M.; Sawamoto, M. *J. Polym. Sci., Part A: Polym. Chem.* **1999**, *37*, 3003.

(22) Percec, V.; Barboiu, B.; Neumann, A.; Ronda, J. C.; Zhao, M. *Macromolecules* **1996**, *29*, 3665.

(23) Moineau, G.; Granel, C.; Dubois, Ph.; Jérôme, R.; Teyssié, Ph. *Macromolecules* **1998**, *31*, 542.

(24) Petrucci, M. G. L.; Lebuis, A.-M.; Kakkar, A. K. *Organometallics* **1998**, *17*, 4966.

(25) Lecomte, Ph.; Draiper, I.; Dubois, Ph.; Teyssié, Ph.; Jérôme, R. *Macromolecules* **1997**, *30*, 7631.

(26) Kotani, Y.; Kamigaito, M.; Sawamoto, M. *Macromolecules* **1999**, *32*, 2420.

(27) Ida, H.; Kamigaito, M.; Sawamoto, M. *Polym. Prepr. Jpn.* **1998**, *47* (7), 1271.

(28) Bandts, J. A. M.; van de Geijn. P.; van Faassen, E. E.; Boersma, J.; van Koten, G. *J. Organomet. Chem.* **1999**, *584*, 246.

(29) Besides the iron halides, iron dithiocarbamates $\{\mathrm{Fe[SC(S)NR_2]_3}$; R = Et, $\mathrm{C_6H_5CH_2}\}$ are effective in living radical polymerization of styrene in the presence of radical initiator like 2,2′-azobis(isobutyronitrile). Nishimura, M.; Kamigaito, M.; Sawamoto, M. *Polym. Prepr.* (*Am. Chem. Soc., Div. Polym. Chem.*) **1999**, *40* (2), 470.

(30) Kotani, Y.; Kamigaito, M.; Sawamoto, M. *Macromolecules* **1999**, *32*, 6877.

(31) King, R. B.; Stone, F. G. A. *Inorg. Synth.* **1963**, *7*, 99.

(32) Fischer, E. O.; Moser, E. *Inorg. Synth.* **1971**, *12*, 36.

(33) Susuki, T.; Tsuji, J. *J. Org. Chem.* **1970**, *35*, 2982.

(34) Davis, R.; Durrant, J. L. A.; Khazal, N. M. S.; Bitterwolf, T. E. *J. Organomet. Chem.* **1990**, *386*, 229.

(35) Elzinga, J.; Hogeveen, H. *J. Org. Chem.* **1980**, *45*, 3957.

(36) Kotani, Y.; Kamigaito, M.; Sawamoto, M. *ACS Symp. Ser.*, in press.

(37) Ando, T.; Kamigaito, M.; Sawamoto, M. *Polym. Prepr. Jpn.* **1999**, *48* (8), 1726; *Macromolecules*, submitted.

(38) Onishi, I.; Baek, K.-Y.; Kotani, Y.; Kamigaito, M.; Sawamoto, M. *Polym. Prepr. Jpn.* **1999**, *48* (2), 136.

(39) Curran, D. P.; Bosch, E.; Kaplan, J.; Newcomb, M. *J. Org. Chem.* **1989**, *54*, 1826.

MA991990F